PENTA
shows you
how to
increase
productivity
by getting
the maximum
from the minimum

Productivity gains in a typesetting business occur when you get more output for the same (or less) effort than previously. Ways of measuring gains in productivity vary. You can look, for example, at keystrokes per operator hour; characters per phototypesetting hour; pages per light table hour; corrections per operator hour, etc. The main point is that outputs (pages, keystrokes, characters, etc.) are measured against input mechanisms (equipment, operators, etc.). The greater the output, the more the productivity. Gains in productivity need to be measured in terms of distance from a standard, or as intervals on a fixed scale. Say, for example, that an operator was, on average, keyboarding 90 wpm. New equipment was installed, and the number of words keyboarded increased to 110. The productivity gain is 20 wpm, or about 22%.

Increasing output is, however, no easy matter, as shop managers have been discovering over the last century or so. Early scientific management methods (the early time and motion studies) took the task, analyzed its physical components (movements, work flow, tools or machines), and reduced the amount of human effort that went into accomplishing that specific task. Later, human relations proponents discovered that increases in employee morale could contribute to increases in productivity. But, even the most highly motivated employee working at the best-defined task in the best-supervised plant quickly reaches optimal output — which might not be significantly higher than average output.

The enormous gains in productivity that are now within reach of many industries are accomplished by a third revolution in industrial perspective — by automation. The electronic revolution that has occurred since World War II — the advent of computers, the development of reliable mainframes, followed by dedicated minis, and, most recently, the incredible micros — has opened up whole new vistas for gains in productivity. Basically, in the typesetting industry, these gains can be looked at along two major dimensions:

1) *decreased keyboarding* (a decrease in physical input by human operators) due to electronic capabilities such as OCR, disk storage, elimination of re-keyboarding, minimizing resetting for corrections, etc.
2) *increased processing speeds* (an increase in the speed with which text — captured keystrokes — can be processed) due to electronic manipulation of stored characters, with a net result of more output per input operator.

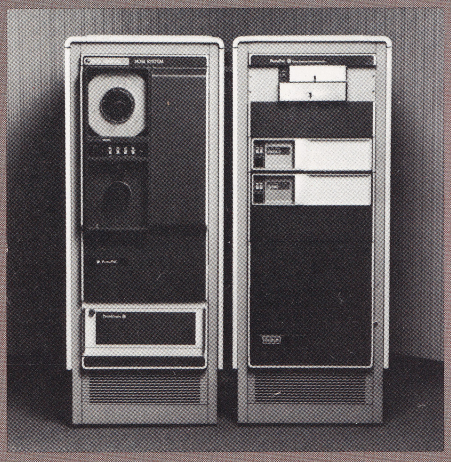

At Penta Systems International, we are dedicated to the proposition that the successful business in today's environment must produce the maximum from the minimum. That is how we've developed our own strategic plans. And why we are so sensitive to our customers' needs for improving their productivity. With the skyrocketing costs of labor, energy and materials, a philosophy of maximizing output is essential for survival, as is the need to maximize return on investment, opportunities in the marketplace, and profits. And, since automation is one of the few commodities that is costing less today than it did five years ago, automation is an increasingly attractive way of ensuring maximal gain from the minimum.

Hence Penta has, over the last 12 years, developed an automated composition system which, once installed, will help your business maximize its potential. In other words, Penta spells productivity gains for the typesetting enterprise. And we can prove it.

The following specific examples will show you more clearly what we mean by increasing productivity. The best way, however, for you to gain an appreciation of Penta's contribution to productivity is to see a hands-on demonstration of our system. At the demo, we will encourage you to pick a "productivity problem" you're familiar with, or maybe one that you think would have any automated system beat — and we'll take pride in showing you how a Penta application of the latest technology combined with the deepest craft knowledge will work to solve that problem.

Here are some examples to whet your appetite for a demonstration — or a system.

1. Input

The productivity of the average individual operator is increased when he or she is using a Penta system because, by contrast with other automated typesetting systems, Penta has streamlined the following basic system features: commands and access.

The heart of the Penta system — its software — features

- commands that are simpler and more logical to use, allowing operators to work with more confidence, and fewer errors
- commands that are task-specific, rather than combinations of non-specific commands which result in cumbersome keyboarding to manage even minor exceptions
- the number of formats employed in the Penta system, and the way they are used, give our system a uniquely powerful formatting capability
- *within* commands, Penta deploys automation, with resultant reduction in formatting time of up to 50%. For example, in setting a shape, the depth, not each specific indent, is specified. Using the variables program, the system — not the operator casting off characters — lines up the indents so that they are properly aligned vertically. In much less time.
- tabular matter is set without lengthy operator calculations and interruption to work flow.

Another major contributor to Penta productivity is that the system is designed for direct keyboarding to a large disk, accessed directly by the system itself for automated text processing and pagination, or by an editing terminal operator for editing. The elimination of movement of floppy disks or paper tapes from work station to work station in itself contributes to productivity gains.

Further, by emphasizing simplicity, Penta has succeeded in decreasing the proportion of commands to text. The result is fewer errors, a shorter correction cycle, easier access during editing — and subsequent gains in production output per operator.

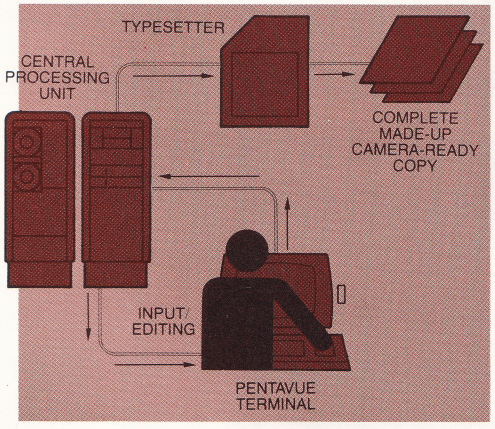

With a Penta System, movement between the PentaVue terminal (input), CPU, PentaVue terminal (for editing), back to CPU and to phototypesetter (output) is completely electronic and automated.

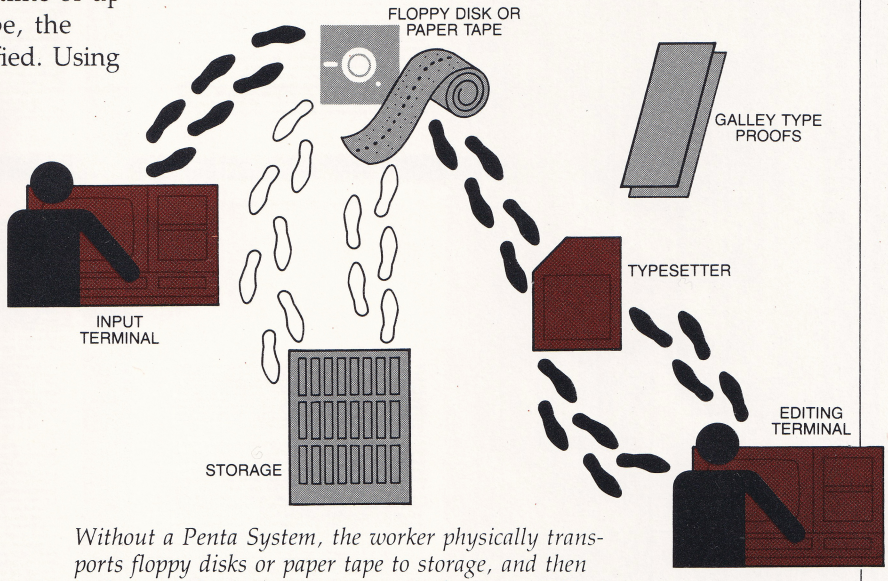

Without a Penta System, the worker physically transports floppy disks or paper tape to storage, and then back out to the typesetter; paper proofs are carried back for editing and back to the typesetter for production of galley proofs.

2. The Correction Cycle

The correction cycle, foreshortened by the simplicity of the Penta system's commands and by direct disk access for editing, is further reduced by our exclusive line numbering feature. The greater the copy length, the more efficiency gains can be expected by using our pinpoint scrolling feature. This Penta exclusive is faster and simpler to use than the ordinary scrolling or search field method that other systems use. The productivity gains made possible by this deceptively simple program translate into your operator being able to locate the error, make the correction, and move on to the next correction long before the operator of a different system would even have established a unique search field.

If your work involves books, journals, manuals, or magazines, the pinpoint scrolling feature alone can give you substantial productivity gains, saving you operator time and scheduling problems — and increasing customer or editor satisfaction with the entire composition process you can offer.

3. Automated Pagination

The 21 pages of complex text matter, including math formulae, indention, and pi characters (shown on this spread) took *seven minutes* to set and paginate. Manual paste-up of these same pages would have taken *two to three hours.*

The steps needed to process the text from captured keystrokes to pages utilize the following Penta programs:

- *Read Program,* which converts the captured keystrokes to Penta language, numbers the lines, sets up the file, and activates the file management system
- *Hyphenation and Justification Program,* with command verification
- *Pagination Program*
- *Output Program,* which converts the text from Penta language to the language of the phototypesetter.

Progress in Cholinergic Biology: Model Cholinergic Synapses, edited by I. Hanin and A. M. Goldberg. Raven Press, New York © 1982.

Superior Cervical Ganglion: Physiological Considerations

Donald A. McAfee

Introduction	191
Historical Overview	192
The Preparation	193
Dissection	195
In Vitro Conditions	195
Electrophysiology	197
Application of Electrophysiological Techniques	201
Bipolar Recording	201
Sucrose Gap	202
Intracellular Measurements	207
Summary and Conclusions	209
References	209

INTRODUCTION

The superior cervical sympathetic ganglion is well established as a model preparation for the study of cholinergic synapses. Indeed, it is probably second in popularity only to the neuromuscular junction for such studies. The ganglion can be studied *in situ* or excised and maintained *in vitro* for hours and even days. It is simple in gross stucture, having well-defined input and output nerves emanating from its body. It is relatively homogenous in cellular composition, with the input cholinergic axons terminating on adrenergic cell bodies and dendrites. This ganglion is appropriate for neurochemical studies, and the amount of tissue available is directly related to the size of the animal. It is structurally well suited for electrophysiological measurements and has long been used as a model for pharmacological studies (40), developmental neurobiology (2), and more recently as a source of primary cell tissue culture (36).

The superior cervical ganglion is not only a model cholinergic synapse but is in general a versatile nervous system preparation. Although the synapses in this ganglion are primarily cholinergic, there is a multiplicity of pre- and postganglionic receptors to biogenic amines, amino acids, and even peptides. It is therefore suitable for studying the release and reception of acetycholine (ACh) and the modulation of this process by other neurotransmitters and neurohormones. In addition, there is evidence of adrenergic synapses in the ganglion, and it is probable that other

neurotransmitter synapses may be demonstrated in the future (7,31). Thus, it is more than just a simple model cholinergic synapse.

Numerous reviews which recount important aspects of ganglionic chemistry and biology have been published (3,13,20,24,39). Kuba and Koketsu (28) published an especially comprehensive review which covers the cellular physiology of amphibian as well as mammalian sympathetic ganglia. Hence this chapter is not intended as a review. Instead, it is intended to introduce the scientist who is unfamiliar with the superior cervical ganglion to the virtues of this preparation as a model cholinergic system.

HISTORICAL OVERVIEW

It is to be expected that a useful preparation such as the superior cervical ganglion would have a long history. In fact, it was among the first nervous tissues used to test the theory of chemical synaptic transmission. Feldberg (18), using a paradigm similar to Leowi's demonstration of *vagustoff,* was able to show ACh release following preganglionic stimulation to the ganglion. In an elegant series of experiments, Feldberg clearly demonstrated that cholinergic synapses activated nicotinic responses distinct from previously known muscarinic responses. He proved that release occurred from presynaptic fibers and not from postsynaptic cells (19).

These pharmacological approaches were complemented by early electrophysiological studies. Sir John Eccles, still somewhat uncertain as to the validity of the idea of cholinergic synaptic transmission, began a series of studies through which he gradually came to the conclusion that ACh released from preganglionic terminals depolarized and caused the postganglionic neurons to fire (15,16). Using primitive electronics, a high-voltage amplifier coupled to the recently invented cathode ray tube, he was able to get records of remarkable fidelity. Eccles obtained synaptic potentials from surface recordings of curarized ganglia and described slow potential processes which still remain the subject of intense study. These early investigators of the superior cervical sympathetic ganglion examined and identifed the essential properties of cholinergic transmission as we know them today. In fact, most of this information was collected before the skeletal neuromuscular junction became a recognized model for synaptic transmission.

Subsequent to these pioneering studies, the superior cervical sympathetic ganglion remained in the armamentarium of the pharmacologist, but the skeletal neuromuscular junction became the primary preparation for quantitative physiological studies of cholinergic transmission. One reason for this is that intracellular measurements can be routinely made at the neuromuscular junction; whereas penetration of postganglionic neurons with microelectrodes is considerably more difficult. However, early studies demonstrated that the electrophysiology of postganglionic neurons is similar to that of spinal neurons. The first comprehensive description of the passive and active membrane properties of sympathetic neurons was produced by Perri et al. (37), but this was 15 years after the first records of intracellular responses were published by Rosamond Eccles (17). Although progress has been slow, intracellular electrophysiology has become common if not routine for sympathetic ganglia.

The current view of ganglion physiology is superficially very simple. Preganglionic discharge results in the release of ACh, which in turn acts on nicotinic receptors in the postganglionic neuron membrane to increase permeability to Na^+ and K^+. The release processes appear to have characteristics similar to those of motor neurons at the skeletal neuromuscular junction (46). However, nicotinic transmission in ganglia has significantly different pharmacology from that of the muscle. For instance, the potent muscle antagonist α-bungarotoxin does not affect ganglionic transmission (8,14). Further, hexamethonium ions are more potent antagonists of nicotinic responses in the ganglion than in skeletal muscle. It is probable that the channel (or ionophore) as well as the receptor are targets of different pharmacological agents in these neurons (Spivak and Albuquerque, *this volume*).

There appear to be two small but potentially important synaptic responses which follow nicotinic discharge of the postganglionic neuron (31). These responses are slow in onset and consist of a slow inhibitory postsynaptic potential (IPSP; hyperpolarization) lasting 3 sec, followed by a slow excitatory PSP (EPSP; depolarization) of 30 sec duration. The slow EPSP arises from activation of muscarinic receptors by ACh released from preganglionic terminals. The slow IPSP is hypothesized to result from the action of a catecholamine released by an interneuron intercalated between pre- and postganglionic neurons. These interneurons may be the small intensely fluorescent (SIF) cells which are thought to respond via muscarinic receptors to preganglionic cholinergic input (44). There is a network of purported catecholamine-containing terminals throughout the ganglion which have been hypothesized to originate from dendrites or from recurrent collaterals of adrenergic postganglionic neurons (10,27). However, the hypotheses of catecholamine transmission in the ganglion have been questioned by various investigators and remain the subject of vigorous controversy and experimentation (13,22). In summary, although cholinergic mechanisms are well characterized, the ganglion is not established as a model for catecholamine transmission.

THE PREPARATION

The superior cervical sympathetic ganglion resides in the carotid sinus, which lies deep and medial to the angle of the jaw (Fig. 1). The cervical sympathetic nerve, which provides most of the input, is in the carotid sheath and is composed largely of axons which originate from cholinergic neurons in the intermediolateral cell column of the thoracic spinal cord. This mixed myelinated and unmyelinated nerve enters the posterior pole of the ganglion, and each preganglionic axon divides into numerous branches before terminating on postganglionic neurons. The cervical sympathetic nerve probably also contains some axons from postganglionic neurons in the inferior cervical ganglion and tiny accessory ganglia along the cervical sympathetic nerve. It is not clear to what extent these axons or their collateral branches terminate in the ganglion, but it is likely that most course through the ganglion and travel with other postganglionic axons to innervate effectors in the head.

FIG. 2. Arrangement for bipolar stimulation and recording from the superior cervical ganglion. **Top:** A pair of platinum wires on the cervical sympathetic nerve is coupled to a pulse generator (stimulator). The polarity is adjusted so that the negative lead (cathode) is nearest the body of the ganglion. Responses to anodal stimulation have higher thresholds and longer latencies. An identical set of electrodes on the internal carotid nerve is capacity coupled to a differential amplifier. The amplifier frequency response should be 2 Hz to 5 KHz. The amplifier should attenuate by 100,000:1 (100 db) a 60-Hz signal applied to both input leads at the same time (common mode). **Bottom:** An arrangement whereby the nerves are sucked up into a tube containing one of the bipolar leads. This submersible arrangement allows for a more stable interelectrode impedance for long periods of stimualtion and recording.

This set-up will be mechanically and electrically stable with a sufficient interelectrode impedance to allow for low-current stimulators and high signal to noise ratio recordings. These procedures are especially suitable for studies of cholinergic neuropharmacology that require stable recording conditions for several hours. Supermaximal stimulation of the cervical sympathetic nerve should occur at less than 10 V (50 mA source), generating a compound action potential in the internal carotid nerve greater than 1 mV. The amplitude of the compound action potential is a function of the number of fibers discharging and the synchrony of their discharge. Consequently, it may be important to integrate the discharge with time in order to determine the basis for the change in response amplitude. For example, increasing the conductance distance reduces the response amplitude but proportionately broadens the period, as the same number of fibers are conducting action potentials.

Sucrose Gap

The sucrose gap approach is employed when DC or slow potentials are to be recorded, or when it is important to have a monophasic compound action potential. Because changes in the average resting potential of a population of neurons can be measured, the sucrose gap technique has been referred to as a "poor man's microelectrode." In simplest terms, the sucrose or air gap is employed to reduce the

short circuit between the recording electrodes in the bathing solution (Fig. 3). The ganglion is inserted into the pregap chamber, and the internal carotid nerve is threaded into rubber gaskets and through the sucrose gap into the postgap chamber. The pre- and postgap chambers contain Locke solution, which flows out and over a nonpolarizing calomel reference electrode. As each chamber is isopotential, the potential across the gap arises from the interface between the Locke and sucrose solutions. The narrow lumen of the rubber gaskets is adjusted by varying their compression for a snug fit around the internal carotid nerve. The sucrose-Locke interface is now limited to only the interstices of the internal carotid nerve. This feature, together with a precisely measured and controlled solution flow to each chamber, greatly reduces junction potential drift and solution change artifacts. In short, the gap potential is really a measure of potential difference along a segment of the internal carotid nerve. For this reason, there may be important differences in the origin of signals recorded by the sucrose gap from those recorded by microelectrodes placed in the cell body of single postganglionic neurons.

The sucrose gap is most convenient for rabbit ganglia, because of their size, but a comparable version using an air gap has been used successfully on rat ganglia, which are considerably smaller (9). In general, this approach, although more involved than simple bipolar techniques, presents exceptionally stable recording conditions suitable for continuous monitoring of the effects of pharmacological agents on ganglionic physiology. It is the principle method by which the slow synaptic potentials have been studied.

Intracellular Measurements

The most direct means of recording transmembrane potentials is to place the electrodes with one on each side of the neuronal membrane. Although this approach samples from only one cell, it is the most powerful means for determining and quantifying biophysical mechanisms underlying electrophysiological responses. Unfortunately, this approach is technically difficult, even for the very experienced investigator; it requires a considerable investment in equipment and manpower and is as much an art as it is a science.

The first step in achieving a reasonable success rate for intracellular penetrations is to mechanically stabilize the set-up. This involves a high mass table with at least some vibration isolation. The experiment chamber and the platform which supports it should be rigid, with low mass superfusion tubing and electrical leads. In fact, it is the "plumbing" which often causes problems during the experiment. The flow and level of the superfusate in the experiment chamber should be constant. There should be enough convection to eliminate stagnant regions and ensure rapid mixing of the bath. The ganglion may be secured by first slitting the capsule to expose the desheathed surface and then pinning down the tough capsule rather than the more friable ganglion tissue.

It seems that once the preparation is mechanically stable the most critical part of the experiment is the quality of the microelectrode. The finer the electrode, as

judged by high electrode resistance, the higher the cellular input impedance and the longer the duration of impalement. Fiber-filled glass capillaries are required since they simplify the task of filling fine pipettes with electrolyte or drugs. There is nothing particularly crucial in the design of the electrode puller or micromanipulator.

It is possible to impale single postganglionic neurons by blindly poking the electrode into the ganglion with little or no optical aid. However, the magnification achieved by a compound microscope allows one to aim a microelectrode at a specific

$$Eg = \frac{n(Ee/N)(Rg)}{Rg + (Re/N)}$$

The voltage Eg across the gap would be equivalent to the electronic potential of a single neuron only when all the axons generate the same electrotonic signal. This assumes that each postganglionic neuron has the same electrotonic conduction distance, an unlikely condition. However, it is clear that the magnitude of the response to submaximal stimulation is directly proportional to the number of axons generating an electrotonic signal. The source impedance (Re) is greatly reduced by the multiple axons, making it easier to achieve an adequate external resistance (Rg) in the sucrose gap.

The above equation can be expressed in terms of the soma-dendritic (Es) potential, attenuated by electrotonic decrement down the axon, as well as in terms of the components in the model which contribute to the total source impedance.

$$Eg = \frac{Es\,[Rm/(Rm + Rs + Ra)]\,(n/N)(Rg)}{Rg + 1/N\,(Ri + Rp + [Rm(Rs + Ra)/(Rm + Rs + Ra)])}$$

Each of the resistance values is dependent on the dimensions of the neurons and the physical arrangement of the apparatus. The equation can be expressed in terms of resistance per unit length and solved for the fraction of somal potential measured across the sucrose gap (see Table 1 for definition of the symbols.):

$$Eg/Es = \sum_{d = 50\ \mu m}^{D = 2.5\ mm} \frac{[(r_m/d)(Rs + r_a d + r_m/d)][n/N][Rg]}{Rg + 1/N(r_a w + [(r_a r_m)/(r_a Lp + r_m/Lp)] + [(r_m/d)(Rs + r_a d)/(r_m/d + r_a d)])}$$

Each ganglionic neuron in the population may have a unique electrotonic conduction distance, and those near the gap contribute more signal than those further away. In rat and rabbit ganglia, the somata which contribute axons to the internal carotid nerve are located in the cephalic end of the ganglion such that the maximum electrotonic conduction distance is about 2.5 mm, whereas the minimum is assumed to be 50 μm. In lieu of a known distribution function, we evaluated the above equation assuming that the somata are uniformly distributed within these limits in groups at 50-μm intervals. There may be as many as 55,000 postganglionic neurons in the rat, but less than half send axons out the internal carotid nerve (47). Therefore we assumed 480 neurons in each group for each 50-μm interval for a total of 24,000 (Table 1).

The above equation can be readily evaluated on a programmable calculator or computer by iterative solutions for incremented values of d. However, it is easily

TABLE 1. *Sucrose gap parameters*

Parameter	Abbreviation and value
Measured values	
Membrane resistivity (37)	$r_m' = 2{,}000\ \Omega\ cm^2$
Axoplasmic resistivity (37)	$r_a' = 100\ \Omega\ cm$
Soma-dendritic input resistance (35)	$Rs = 50 \times 10^6\ \Omega$
Length of postgap nerve	$Lp = 3 \times 10^{-1}\ cm$
Width of gap	$w = 3 \times 10^{-1}\ cm$
Total no. of axons spanning gap (21,47)	$N = 24{,}000$
Average axonal diameter (21)	$Di = 10^{-4}\ cm$
Maximum conduction distance	$D = 0.25\ cm$
Variables (min.–max)	
Electrotonic conduction distance	$d = 50 \times 10^{-4} - 0.25\ cm$
No. of active somata in each 50 μm segment	$n = (0–480)$
Computed values	
	$Ra = r_a'd/(\pi\ (Di/2)^2) = r_a d = (1.3 \times 10^{10}\ \Omega/cm)(d)$
	$Rm = r_m'/(\pi\ (Di)(d)) = r_m/d = (6.7 \times 10^6\ \Omega cm)/d$
	$Ri = r_a w = 3.9 \times 10^9\ \Omega$
	$Rp = (r_a r_m)/(r_a Lp + r_m/Lp) = 2.2 \times 10^7\ \Omega$
	$\lambda = [r_m Di/4r_a]^{1/2} = 0.022\ cm$

simplified. The internal gap resistance ($Ri = r_a w$) dominates the source impedance (Re) term for gaps wider than 0.5 mm. This term is inversely proportional to the number of axons and should be about $10^5\ \Omega$ in most set-ups.

As the resistivity of sucrose is on the order of $10^7 \Omega cm$ (42), Rg should be about $10^8\ \Omega/mm$ in a gap 1 mm in diameter. Thus Rg is likely to be much larger than Re and

$$Eg/Es = \sum_{d = 50\ \mu m}^{d = 2.5\ mm} [(r_m/d)/(Rs + r_a d + r_m/d)][n/N]$$

That is, the gap potential is equivalent to the average soma-dendritic potential attenuated by electrotonic decay and inactive axons. Thus using the values from Table 1, only 11% of the soma-dendritic potential is measured by the sucrose gap when *all* axons are active.

Although soma-dendritic signals are detected by the microelectrode and attenuated in the sucrose gap, signals originating in axons (Ea) are not easily detected by a somal microelectrode. The soma-dendritic membrane has a low impedance relative to the axonal source impedence, such that:

$$Es = Ea\ Rs/[Rs + (r_m r_a)/(r_m/d + r_a d)] = c$$

Thus a potential change that occurs only on the axon 50 μm away from the soma would be 50% attenuated in the soma but would produce a gap potential slightly greater than if the event had occurred in the soma.

Our studies suggest that catecholamines do not affect the resting membrane potential of axons (25). In sympathetic ganglia, norepinephrine produces a hyperpolarization of 0.4 to 0.7 mV measured extracellularly (6,31) and a hyperpolarization of 1 to 6 mV measured intracellularly from postganglionic neurons (6,26). This result is consistent with our calculation that the intracellular potentials should be ninefold greater than the sucrose-gap potential. Brown (6) concluded from his empirical studies that the microelectrode potentials are five to ten-fold greater.

In summary, then, the microelectrode should provide a much better measure of soma-dendritic events than the sucrose gap. However, the sucrose gap would provide larger responses than the microelectrode to events that originate on the axons of the internal carotid nerve. The microelectrode measures only neuronal potentials. The sucrose gap could conceivably respond to potential changes occurring in electrically coupled epithelial cells which span the gap with the internal carotid nerve.

Intracellular Measurements

Although intracellular measurements are the most difficult technically, they actually simplify interpretation of bioelectric records. In contrast to bipolar electrodes, the intracellular microelectrode measures the transmembrane potential *directly.* In addition, it is possible to pass current through the microelectrode and to alter the ionic composition of the bathing media. Thus the investigator has control over the chemical and the electrical driving forces that control ion fluxes. This is a powerful means to determine the ionic mechanisms which underlie membrane potential changes.

Often the act of impaling a neuron causes obvious damage. The magnitude of the action potential, its speed, the input impedance, and the membrane potential will all be unusually low. However, we have had considerable experience recording from hundreds of cells, and we assume that the values listed in Table 2 are characteristic of healthy neurons.

TABLE 2. *Membrane properties of rat postganglionic neurons*

Property	Value	No.
Resting membrane potential	−60 ± 1mV	170
DC input impedance	52 ± 3 m Ω	160
Cell time constant	3.5 ± 0.1 msec	15
Spike amplitude	77 ± 1 mV	170
E_K	89 ± 2 mV	6
P_{NaK}	0.084	Calculated[a]
r_m	2300 Ω cm²	Calculated[b]
C_m	1.5 μF cm⁻²	Calculated[b]

[a]Assumes: normal Locke solution; 20°C; $E_{HAP} = E_K$.
[b]Assumes: neuron surface area = $4.4 \times 10^{-5}\ cm^2$.

A Penta user recently had to repaginate an entire 300 page book because of some author's alterations. The entire job took the Penta system, with its PentaPage optional program, 25 minutes. That, we can safely say, is *fast*. And that kind of speed, especially for jobs that could make the difference between a satisfied customer and a disgruntled customer with a repaging surcharge, is an essential measure of system productivity.

In many mammals, the ganglion is bilobed, or double fusiform, in shape, possibly the result of fusion during ontogeny with the equivalent of the middle cervical ganglion. There are two major postganglionic nerves which exit the ganglion (32). The external carotid nerve exits from the posterior lobe in the middle of the ganglion, and the internal carotid nerve exits from the anterior pole. It is this latter nerve that is usually used for extracellular recordings of postganglionic discharge. These nerves distribute with their respective arteries: the external carotid innervates blood vessels of the face (also eccrine sweat glands in man); the internal carotid nerve enters the cranium, where one branch innervates the pineal body, and others distribute with the oculomotor nerve to innervate the dilator muscles of the iris and the smooth muscles of the nictitating membrane and palpebra (eyelids). In fact, the best sign of a chronic denervation in rats and rabbits is a half-closed eye on the lesioned side. Disturbances in pupillary control are harder to detect since the parasympathetic innervation still provides light reflex responses.

In general, the size and weight of sympathetic ganglia are proportional to the body weight of the animal. The wet weight of the rat superior cervical sympathetic ganglion is about 1 mg, of the rabbit 10 mg, and of the calf about 200 mg. The protein content is approximately one-seventh the wet weight. The rat ganglion contains 35,000 to 55,000 postganglionic neurons innervated by only 2,000 to 7,000 unmyelinated preganglionic fibers. The rat ganglion also contains about 400 SIF cells. There is evidence that these small catecholamine-containing cells function as inhibitory interneurons by generating slow IPSPs. The major cellular element in this ganglion, however, is flattened satellite cells, which appear to surround the neurons and probably account for the diffusional and mechanical barriers within this tissue. Finally, the ganglion is encased in a tough connective tissue sheath, or capsule, with a bulk equivalent to that of the desheathed ganglion (3,21,43,45).

There are some important variations on the above general description. During ontogeny, the coalescence of these ganglia can be observed along the sympathetic chain. Sometimes, if the coalescence is incomplete, the ganglia of rats and rabbits becomes so elongated that a myelinated stalk connects the anterior and posterior lobes. In rabbit ganglia, the internal carotid nerve is highly divided and sometimes forms a plexus around the internal carotid artery, making dissection and desheathing difficult. Finally, it seems that there are some preganglionic cholinergic fibers in the postganglionic nerve. It may be that these axons are from the cervical sympathetic nerve and have passed through the body of the ganglion, giving off collateral branches, to continue on into the postganglionic nerves, perhaps to innervate accessory ganglia anterior to the superior cervical ganglia. Although these fibers are few in number, they provide a unique arrangement whereby stimulation of the external carotid nerve antidromically activates postganglionic neurons in the posterior lobe but orthodromically activates a few neurons in the anterior lobe. This orthodromic activity is very weak, but it is useful for studying subthreshold synaptic activation of postganglionic neurons (12,38).

Dissection

Superior cervical sympathetic ganglia from the rat can be isolated as follows: Decaptaite the rat, pin the head ventral surface up, and make a midline incision from the wound along the trachea into the lower jaw. With blunt dissection, reflect the trachea/esophagus forward and pin it over the nose. This procedure quickly exposes the neck cavity. Hook the cut end of the common carotid artery with a bent insect pin and gently stretch out the artery. The large white nerve which runs with the artery is the vagus nerve (Fig. 1). The artery disappears between two muscles, including the sternomastoid, and these muscles must be spread apart to expose the carotid sinus. The superior cervical sympathetic ganglion lies on the bifurcation of the carotid artery. It is possible to see the sympathetic nerve and the larger vagus nerve. The ganglion may now be freed from the overlying connective tissue and transferred to a tray for superfusion. Here, the ganglion is desheathed by first girdling the capsule in the middle of the ganglion and then spreading and everting the cut edges of the capsule toward each pole, pulling outward over the pre- and postganglionic nerves. If it is necessary to pin the ganglion to some supporting surface, for instance during intracellular recording, the capsule can be slit longitudinally instead of being removed from the ganglion, and the cut edges can be spread apart and pinned. In this fashion, the pins need not pass through neuronal tissue, and the connective tissue of the capsule provides the means with which to grip the ganglion.

Ganglia from other species may be found using the same general landmarks, but a stereomicroscope is handy when mice or neonates are dissected. Cats and rabbits are often used intact and under urethane (1 g/kg body weight) rather than barbiturate anesthesia as barbiturates depress ganglionic transmission. I have routinely used a 50% (w/v) solution of urethane injected into the marginal ear vein of the rabbit. Quick injection of the first 5 ml will sedate the rabbit, and another 5 to 15 ml must be injected for deep surgical anesthesia. It should be injected slowly over 60 sec to avoid respiratory or cardiac arrest. Resuscitation is easily effected by closed-chest cardiac massage.

In Vitro Conditions

Ganglia may be maintained *in vitro* for many hours without obvious detriment to electrophysiological responses. Oxygenated Locke solution is the most common medium for incubating mammalian sympathetic ganglia and has the following millimolar composition: NaCl 136, KCl 5.6, $CaCl_2$ 2.2, $MgCl_2$ 1.2, NaH_2PO_4 1.2, $NaHCO_3$ 20, and dextrose 8.3. This solution is equilibrated with 95% O_2/5% CO_2 to bring the pH up to 7.4 prior to adding the Ca and Mg salts.

It is likely that mammalian ganglia have relatively high metabolic rates simply on the basis of surface area to volume considerations (5,11,39). In order to avoid developing an anoxic core in the isolated tissue, the medium should be flowing or stirred and kept saturated with the O_2/CO_2 mixture. The amount of anoxic core is

Set Fig. 1 Broadside here

directly related to the size of the ganglion and the level of neuronal activity, and it is especially sensitive to temperature. Thus it may be advantageous to run experiments at temperatures less than 36°C and to slice ganglia larger than 2 mm in diameter. In general, it is best to fashion a simple chamber with a shallow trough to channel a continuous flow of Locke solution (1 to 2 ml/min) over the ganglion. Most procedures, including electrophysiological measurements, can then be carried out during uninterrupted superfusion.

Electrophysiology

There are no real standard or conventional procedures for electrophysiological measurements. Such statements in methods sections usually mean that one of three general approaches were used, and that there was nothing obviously critical in the specific implementation of that approach. The most common measurement is of compound action potentials obtained with bipolar precious metal electrodes. Secondly, it is possible to obtain DC and slow potentials by recording from the surface of the ganglion with nonpolarizing bipolar electrodes. The magnitude of the recorded potentials is enchanced by an air or sucrose gap (42) between the electrodes. Lastly, single postganglionic neurons and even satellite cells may be impaled by fine glass pipettes to record their transmembrane potentials.

Bilpolar Recording

The bipolar recording technique is easily learned by the student and nonelectrophysiologist. The simplest procedure is to fashion a pair of platinum wires into hook electrodes (Fig. 2). These electrodes can be used for stimulating and recording from virtually any tissue. The key to stable electrophysiology is to maintain a constant interelectrode impedance for the duration of the experiment. The disadvantage of these electrodes is that they are badly short-circuited by the bathing media. One must lift the nerves out of the bath with the hook electrodes to make the measurements. If the procedure lasts more than a minute, the tissue must be protected from dehydration. It is possible, though difficult, to make repetitive measurements over a period of time by submerging the preparation between measurement trials. Without special care, there will be variations in the amount of short-circuiting Locke solution adherent to the tissue with each trial. Alternatively, petroleum jelly thinned with mineral oil can be applied from a syringe to cover the exposed nerve, allowing measurements to be made for several hours. When using petroleum jelly as a vapor barrier, care must be taken to prevent disturbances that allow oil to collect between nerve and electrode, which creates a noisy high-impedance signal source.

Long-term quantitative observations are more easily obtained with suction bipolar electrodes (Fig. 2). These electrodes are more complex to construct and are less versatile than hook electrodes but may be immersed in the superfusate with the preparation. If routine measurements are to be made from about the same-sized ganglion, then electrodes can be designed so that they fit snugly around the nerve.

neuron to acheive controlled penetration. The Aus Jena microsurgical apparatus is an ideal system for such intracellular studies because of its fixed stage with focusing optics. The resolution with long working distance objectives is adequate when Köhler illumination is used. Hoffman interference contrast optics can be used to further enhance visualization of neurons in fresh unstained tissue during microelectrode procedures.

APPLICATION OF ELECTROPHYSIOLOGICAL TECHNIQUES

Bipolar Recording

The suction electrode set-up provides an excellent and versatile tool for studying the neurobiology of the ganglion. Repetitive preganglionic stimulation (at physiological frequencies of 3 to 30 Hz) for 30 sec (3) results in metabolic changes in the tissue including a twofold increase in cyclic AMP and a fivefold increase in cyclic GMP. Recording the postsynaptic response is the only independent means of determining that the ganglion is functioning properly. Furthermore, if agents which alter synaptic transmission are used, their efficacy can be verified and unexpected nonspecific effects observed. For instance, atropine does not block transmission of compound action potentials but does block the increase in cyclic AMP following repetitive preganglionic stimulation. This suggests that muscarinic cholinergic responses are in some way related to cyclic AMP metabolism (34). Synaptic activity also increases glucose and oxygen consumption (29), phospholipid turnover (30), and $^{45}Ca^{2+}$ uptake (4).

Cyclic nucleotides and other metabolites can be studied by immunocytochemical means (3). Instead of homogenizing the tissue at the end of the stimulus period, it is possible to freeze and then slice the tissue. Incubation of the ganglion slices with specific antibodies and fluorescent tags allows identification of the cell type in which cyclic nucleotide levels change (M. Ariano, *personal communication*).

In many respects the behavior of nicotinic cholinergic transmission in the ganglion is similar to that in the neuromuscular junction. It is possible to demonstrate synaptic depression in the ganglion (33,34). It is particularly interesting that Ca^{2+} greatly

FIG. 3. Sucrose gap preparation and scale drawing of the apparatus. A rabbit ganglion spans four Plexiglas chambers (stimulus, pregap, sucrose, and postgap). Test Locke solution from one of several reservoirs flows through (1 to 2 ml/min) the pregap chamber and onto a calomel (pH reference) electrode. Similarly, Locke solution flows through (0.5 to 1 ml/min) the postgap chamber and onto a second calomel electrode. Isotonic (315 mM) sucrose flows through (0.3 ml/min) a narrow chamber sandwiched between the pre- and postgap chambers and is sealed by two silicon rubber gaskets. These gaskets were fashioned from gas chromatograph septa (¼ inch) by slicing off a thin disk and punching a lumen for the internal carotid nerve in its center with a 20-gauge needle. The gaskets can be compressed by adjusting the screws which clamp the pre- and postgap chambers to the sucrose chamber. Increasing the compression causes the lumen of the gasket to be narrowed, making a seal around the nerve sufficient to restrict the sucrose/Locke interface to the interstices of the nerve. The potential difference across the gap is recorded differentially. The postgap chamber essentially functions as a reference electrode, as action potentials cannot propagate through the sucrose solution.

affects the amount of synaptic depression. Many investigators hypothesize that most of the ACh in the terminal is not available for immediate release. If the small pool of readily available ACh is depleted faster than it is replenished, synaptic depression occurs. Higher-frequency stimulation or increased release by elevated Ca^{2+} increases the amount of synaptic depression during the stimulus train. Recently we observed that norepinephrine and adenosine specifically antagonize synaptic depression. Thus bipolar recordings form one approach for our studies of presynaptic receptors which modulate cholinergic transmission (34).

In summary, the suction electrode techniques are convenient to implement and are valuable adjuncts to studies which correlate biochemical and physiological responses. They are also a valuable means of studying cholinergic transmission at neuron-neuron synapses, a system more comparable to the central nervous system (CNS) than the neuromuscular junction.

Sucrose Gap

I have employed the sucrose gap in studies of synaptic or nonpropagating potentials (46). Because of possible flow and mixing artifacts which result in DC drift, this preparation is probably less reliable than microelectrodes for recording DC or resting membrane potentials. Although it is clear that the sucrose gap technique is not as good as the microelectrode technique, there is too much mystique and misunderstanding concerning what this technique measures. I present here a simple but quantitative analysis useful for defining the critical parameters of this recording system and for interpreting the records.

Single Axon Model

The postganglionic neuron is represented in Fig. 4A as a single variable-voltage source applied to a network of passive conductances. The resting membrane potential is not indicated because it is the same on both sides of the gap. Junction potentials are ignored as they should be constant during the experimental manipulations. The capacitance is neglected for slowly changing synaptic or drug-induced potentials. The variable-voltage source, then, is intended to represent a receptor-mediated event occurring in the soma-dendritic membrane.

The network can be rigorously reduced in complexity by employing Thevenin's theorem (23): *The potential at any point on the membrane can be made equivalent to a single parallel voltage source with a series resistor*. Thus the soma-dendritic network, V, R, R′ can be isolated and reduced to the voltage drop (Es) in series with Rs, a resistance equivalent to the parallel resistances R and R′ (Fig. 4B). This is the voltage and input resistance measured by a microelectrode inserted in the soma.

FIG. 4. A: An electrical analog for measurements of membrane potential by a somal microelectrode and sucrose gap across the axon of a postganglionic neuron. A slow voltage event (ΔV) in the soma-dendritic membrane produces a transmembrane potential change (Es) across resistors *R* and *R′*. This potential is electrotonically conducted through axoplasmic (Ra) and axolemma (Rm) resistances and generates a potential change (Ee) in the axon at the sucrose/Locke interface. This electrotonic potential (Ee) is applied to a resistor network which includes the internal (Ri) and external (Rg) resistance of the axon in the gap as well as the postgap axon membrane (Rm′, Ri′). The potential across the gap (Eg) can be measured and related to the somal potential change (Es) by the network analysis described in the text. **B:** Successive reduction of the above network is accomplished by Thevenin equivalent circuits to one where the potential across the sucrose gap (Eg) is a function of an electronic potential (Ee) and the divider network *Rg* and *Re*. **C:** Equivalent circuits for multiple axons spanning the sucrose gap where N is the total number of axons and n is the number of axons generating electrotonic potentials. $(Ee)_n$ and $(Re)_N$ represent the electrotonic potential and resistance generated by any one axon. All axons are assumed to have the same properties.

$$Es = \frac{\Delta V\ R'}{(R + R')} \quad \text{and} \quad Rs = \frac{(R)\ (R')}{(R + R')}$$

This equivalent circuit is successively reduced in Fig. 4B. Thus the soma-dendritic potential, electrontonically conducted to the gap, is decremented by Ra and Rm such that:

$$Ee = \frac{Es\ Rm}{(Rs + Ra + Rm)} \quad \text{and} \quad R_A = \frac{Rm(Rs + Ra)}{(Rs + Ra + Rm)}$$

The potential across the gap (Eg) is easily derived from the next Thevenin equivalent:

$$Eg = \frac{Ee\ Rg}{Rg + Re}$$

where $Re = Re + Rp + R_A$

$$Re = Ri + \frac{(Ri')\ (Rm')}{(Ri' + Rm')} + \frac{(Rm)\ (Rs + Ra)}{(Rm + Rs + Ra)}$$

Usually the external gap resistance (Rg) is considered to be much larger than the electronic resistance (Re) so that the gap potential (Eg) is 80 to 95% of the electrotonic potential (Ee). It is clear, then, that the gap potential will always be smaller than the soma-dendritic potential or that which is measured by the microelectrode.

Multiple Axons—Internal Carotid Nerve:

The analysis is significantly altered by multiple axons spanning the gap, as can be seen in Fig. 4C. These axons represent shunts which decrement the potential applied to the gap by any one axon. The current generated by one axon can be returned through the gap by the averaged internal and membrane impedances of the N axons of the internal carotid nerve. Thus an axon with a source impedance Re drives a load impedance of $Re/(N-1)$, where N = 24,000 axons in the rat. However, as more axons become active, their electrotonic potentials are added together. Thus the gap potential generated by n axons in a nerve containing N axons is:

The postganglionic neuron exhibits a number of specific ion conductances (Table 3). This means simply that the membrane permeability to certain ions is characterized in different but specific ways. It is common to imagine that the structural basis for these ion conductances is a set of membrane channels with specific biophysical and pharmacological properties. For instance, Na^+ permeability is briefly increased by depolarization. The conductance change results in an inward current and the rising phase of the spike but is blocked by tetrodotoxin. Depolarization also increases permeability to Ca^{2+} and K^+. The Ca^{2+} conductance is much smaller and is antagonized by divalent cations.

There are several specific K^+ conductances which have been described in invertebrate neurons that also appear to be present in mammalian postganglionic neurons. The largest K^+ conductance is noninactivating, responsible for the falling phase of the spike, and generates most of the conductance at the resting potential. However, there is a smaller K^+ conductance at the resting potential which is inactivated by depolarization called the "A" current in molluscan neurons. This conductance was recently observed in primary cultures of rat and chick sympathetic neurons (Pope and O'Lague, *personal communication*).

Some conductances are controlled by means other than transmembrane voltage. Ca^{2+} influx can trigger a K^+ conductance which results in a long-lasting hyperpolarizing afterpotential (35). There is receptor-mediated control of ionic conductances. It is well know that γ-amino acid butyric acid (GABA) increases Cl^- conductance. Although GABA is not normally released in the superior cervical ganglion, there are GABA receptors which, when activated, cause depolarization of the neurons. Postganglionic neurons have a high intracellular concentration of Cl^- such that the electrochemical gradient favors efflux (1).

Acetylcholine (ACh) acts as nicotinic receptors to increase permeability to most cations. The nicotinic ionophore/channel does not seem to be especially ion selective. However, recent observations strongly suggest that ACh acts on muscarinic receptors to produce a completely different effect. Muscarinic depolarization of frog sympathetic neurons occurs by a specific decrease in K^+ conductance. This K^+ conductance mechanism for the slow EPSP appears to be distinct from others described above (7).

TABLE 3. *Specific tonic conductances in postganglionic neurons*

Ion	Features/function	Specific antagonist
Na^+ (v)	Quickly inactivates/rising phase of spike	Tetrodotoxin 10^{-7} M
Ca^{2+} (v)	Slowly inactivates/transmitter release, membrane excitability	Cd^{2+}, Mn^{2+} 4×10^{-3} M
K^+ (v)	Noninactivating/falling phase spike	Tetraethylammonium 10^{-2} M
K^+ ($\bar{v}$)	Inactivated by depolarization	4-Aminopyridine ?
K^+ (Ca^{2+})	Activated by Ca^{2+}/hyperpolarizing afterpotenial	Ba^{2+} 3×10^{-3} M
K^+ ($\bar{m}$)	Activated by polarization/slow EPSP	Muscarine 10^{-6} M
Cl (GABA)	Activated by GABA/polarization	Bicuculline 2×10^{-5} M

There are likely to be other neurotransmitters which function to modulate specific ionic conductances. We have evidence that α_2 and adenosine receptors inhibit Ca^{2+} conductance. Peptides such as leutinizing hormone releasing hormone (LHRH) may act on K^+ conductances. However, progress in this field is limited because our characterization of those conductances is qualitative. The frog sympathetic ganglion contains unipolar neurons and has a good geometry for voltage-clamp studies. The voltage-clamp technique is necessary if the magnitude, time course, and voltage sensitivity of these conductances are to be quantified. Biophysical studies of the mammalian multipolar neurons are in progress but are likely to be more complex.

SUMMARY AND CONCLUSIONS

The superior cervical sympathetic ganglion continues to serve as a model nervous system preparation. It is suitable for routine studies requiring easily implemented electrophysiological measurements and metabolic correlates to nervous system function. The multiplicity of receptors in the ganglion (41) makes it especially suitable as a model system for neurobiological research. This preparation should serve well in the future as a transition system between the neuromuscular junction and the brain.

ACKNOWLEDGMENTS

I wish to thank Lloyd Carder and Sharyn Webb for assistance in preparation of this manuscript. My research activities over the years have been supported by the NIH, the NSF, and the American Heart Association.

REFERENCES

1. Adams, P., and Brown, D. (1975): Actions of γ-aminobutyric acid on sympathetic ganglion cells. *J. Physiol. (Lond.)*, 250:85–120.
2. Black, I. B., Coughlin, M. D., and Chochard, P. (1979): Factors regulating neuronal differentiation. *Soc. Neurosci. Symp.*, 4:184–207.
3. Blackman, J. (1974): Function of autonomic ganglia. In: *The Peripheral Nervous System*, edited by J. Hubbard, pp. 257–297. Plenum, New York.
4. Blaustein, M. (1971): Preganglionic stimulation increasing calcium uptake by sympathetic ganglia. *Science*, 172:391–393.
5. Brinley, F. J. (1967): Potassium accumulation and transport in the rat sympathetic ganglion. *J. Neurophysiol.*, 30:1531–1560.
6. Brown, D. A., and Caulfield, M. P. (1979): Hyperpolarizing 'α_2'-adrenoceptors in rat sympathetic ganglia. *Br. J. Pharmacol.*, 65:435–445.
7. Brown, D. A., Censtanti, A., and Adams, P. R. (1981): Slow cholinergic and peptidergic transmission in sympathetic ganglia. *Fed. Proc. (in press)*.
8. Brown, D. A., and Fumagalli, L. (1977): Dissociation of α-bungarotoxin binding and receptor block in the rat superior cervical ganglion. *Brain Res.*, 129:165–168.
9. Brown, D., and Marsh, S. (1975): A very simple method for recording ganglion depolarization. *J. Physiol. (Lond.)*, 246:24–26P.
10. Dail, W., Choudary, S., Barroza, C., Murray, H., and Bradley, C. (1980): The fate of adrenergic fibers which enter superior cervical ganglion. In: *Histochemistry and Cell Biology of Autonomic Neurons, SIF Cells, and Paraneurons*, edited by O. Eränkö, S. Soinila, and H. Paivarinta. Raven Press, New York.
11. Dolivo, M., and Rouiller, C. (1969): Changes in ultrastructure and synaptic transmission in the sympathetic ganglion during various metabolic conditions. *Prog. Brain Res.*, 31:111–123.

12. Douglas, W. W., and Ritchie, J. M. (1956): The conduction of impulses through the superior cervical and accessory cervical ganglia of the rabbit. *J. Physiol. (Lond.)*, 133:220–231.
13. Dun, N. (1980): Ganglionic transmission: electrophysiology and pharmacology. *Fed. Proc.*, 39:2982–2989.
14. Dun, N. J., and Karczmar, A. G. (1980): Blockage of ACh potentials by alpha-bungarotoxin in rat superior cervical ganglion cells. *Brain Res.*, 196:536–540.
15. Eccles, J. (1935): The action potential of the superior cervical ganglion. *J. Physiol. (Lond.)*, 85:179–206.
16. Eccles, J. (1944): The nature of synaptic transmission in a sympathetic ganglion. *J. Physiol. (Lond.)*, 103:27–54.
17. Eccles, R. (1955): Intracellular potentials recorded from a mammalian sympathetic ganglion. *J. Physiol. (Lond.)*, 130:572–584.
18. Feldberg, W., and Goddum, J. (1934): The chemical transmitter at synapses in a sympathetic ganglion. *J. Physiol. (Lond.)*, 81:305–319.
19. Feldberg, W., and Vartiainen, A. (1934): Further observations on the physiology and pharmacology of a sympathetic ganglion. *J. Physiol. (Lond.)*, 83:103–128.
20. Fozard, J. (1979): Cholinergic mechanisms in adrenergic function. In: *Trends in Autonomic Pharmacology, Vol. 1*, edited by S. Kalsner, pp. 145–194. Urban and Schwarzenberg, Baltimore.
21. Gabella, G. (1976): Ganglia of the autonomic nervous system. In: *The Peripheral Nerve*, edited by D. Landon, pp. 355–388. Wiley, New York.
22. Gallagher, J., Shinnick-Gallagher, P., Cole, A., Griffith, W., and Williams, B. (1980): Current hypothesis for the slow inhibitory postsynaptic potential in sympathetic ganglia. *Fed. Proc.*, 39:3009–3013.
23. Grob, B. (1977): *Basis Electronics*. McGraw-Hill, New York.
24. Haefly, W. (1972): Electrophysiology of the adrenergic neuron. In: *Handbook of Experimental Pharmacology*, edited by O. Eichler, A. Farah, H. Herken, and A. Welch, pp. 661–725. Springer-Verlag, New York.
25. Horn, J. P., and McAfee, D. A. (1977): Modulation of cyclic nucleotide levels in peripheral nerve without effect on resting or compound action potentials. *J. Physiol. (Lond.)*, 269:753–766.
26. Horn, J., and McAfee, D. (1980): Alpha-adrenergic inhibition of calcium-dependent potentials in rat sympathetic neurones. *J. Physiol. (Lond.)*, 301:191–204.
27. Kondo, H., Dun, N. J., and Pappas, G. D. (1980): A light and electron microscopic study of the rat superior cervical ganglion cells by intracellular HRP-labeling. *Brain Res.*, 197:193–199.
28. Kuba, K., and Koketsu, K. (1978): Synaptic events in sympathetic ganglia. *Prog. Neurobiol.*, 11:77–169.
29. Larabee, M., Harowicz, P., Steriel, W., and Dolivo, M. (1957): Metabolism in relation to function in mammalian sympathetic ganglia. In: *Metabolism of the Nervous System*, edited by D. Richter, pp. 208–220. Pergamon, New York.
30. Larabee, M., Klingman, J., and Leicht, W. (1963): Effects of temperature, calcium and activity on phospholipid metabolism in a sympathetic ganglion. *J. Neurochem.*, 10:549–570.
31. Libet, B. (1970): Generation of slow inhibitory and excitatory postsynaptic potentials. *Fed. Proc.*, 29:1945–1956.
32. Matthews, B., and Robinson, P. (1980): The course of post-ganglionic sympathetic fibres distributed with the trigeminal nerve in the cat. *J. Physiol. (Lond.)*, 303:391–401.
33. McAfee, D., Henon, B., Horn, J., and Yarowsky, P. (1981): Calcium currents modulated by adrenergic receptors in sympathetic neurons. *Fed. Proc. (in press)*.
34. McAfee, D., Henon, B., Whiting, G., Horn, J., and Yarowsky, P. (1980): The action of cyclic AMP and catecholamines in mammalian sympathetic ganglia. *Fed. Proc.*, 39:2997–3002.
35. McAfee, D., and Yarowsky, P. (1979): Calcium dependent potentials in the sympathetic neurone. *J. Physiol. (Lond.)*, 290:507–523.
36. O'Lague, D. H., Potter, D. D., and Frushpan, E. J. (1978): Studies on rat sympathetic neurones developing in cell culture. I. Growth characteristics and electrophysiological properties. *Dev. Biol.*, 67:384–403.
37. Perri, V., Sacchi, O., and Casella, C. (1970): Electrical properties and synaptic connections of the sympathetic neurons in the rat and guinea-pig superior cervical ganglion. *Pflüegers Arch.*, 314:40–54.
38. Sacchi, O., and Perri, V. (1971): Quantal release of acetylcholine from the nerve endings of the guinea-pig superior cervical ganglion. *Pflüegers Arch.*, 329:207–219.

39. Skok, V. (1973): *Physiology of Autonomic Ganglia*. Igaku Shoin, Tokyo.
40. Volle, R. L. (1975): Cellular pharmacology of autonomic ganglia. In: *Cellular Pharmacology fo Excitable Tissue*, edited by T. Narahashi, pp. 89–140. Charles C Thomas, Springfield, IL.
41. Wallis, D. (1979): The apparent multiplicity of ganglionic receptors. In: *Trends in Autonomic Pharmacology, Vol. 1*, edited by S. Kalsner, pp. 21–57. Urban and Schwarzenberg, Baltimore.
42. Wallis, D. I., Lees, G. M., and Kosterlitz, H. (1975): Recording resting and action potentials by the sucrose-gap method. *Comp. Biochem. Physiol.*, 50:199–216.
43. Wallis, D., and North, R. (1978): Synaptic input to cells of the rabbit superior cervical ganglion. *Pflüegers Arch.*, 374:145–152.
44. Williams, T. H., Black, A. C., Chiba, T., and Bhalla, R. (1975): Morphology and biochemistry of small, intensely fluorescent cells of sympathetic ganglia. *Nature*, 256:315–317.
45. Williams, T., Chiba, T., Black, A., Bhalla, R., and Jew, J. (1976): The SIF cell as a functional dopamine-releasing interneuron, in the rabbit superior cervical ganglion. In: *SIF Cells*, edited by O. Eränkö, pp. 143–162. Government Printing Office, Washington, D.C.
46. Zengel, J., Magleby, K., Horn, J., McAfee, D., and Yarowsky, P. (1980): Facilitation, augmentation, and potentiation of synaptic transmission at the superior cervical ganglion of the rabbit. *J. Gen. Physiol.*, 76:213–231.
47. Zigmond, R. E. (1980): The long-term regulation of ganglionic tyrosine hydroxylase by preganglionic nerve activity. *Fed. Proc. (Symp.)*, 39:3003–3008.

Using (27) and (28) one can easily estimate the order of dropped terms proportional to θ_x and θ_{xx} in eqs. (23) and obtain the solution

$$\phi = \exp\left\{-1\left[\left(1-\frac{a_0^2}{2}\right)t + \frac{\alpha a_0}{2\sqrt{2}}\left(\frac{a_0 x}{\sqrt{2}}\right)\sin 2t\right]\right\} \quad (29)$$
$$\times\, a_0 \operatorname{sech}\left[\frac{a_0}{\sqrt{2}}\left(x + \frac{\alpha}{2}\cos 2t\right)\right]$$

which is valid when $\alpha a_0 < 1$ and $a_0^2 < 1$.[5]

At small α one may try the first in α order corrections in variables μ, ν, χ and ∂ are (see [10]) and related with the inverse method.

The substitution

$$\phi = \sqrt{2}\exp(-it)u(x,\tau)$$

renders eq. (2) into the "standard" form [10]

$$iu\tau + \frac{1}{2}u_{xx} + |u|^2 u = -\frac{\alpha}{2}u_x^* \exp(i\tau) \quad (30)$$

where $\tau = 2t$. The solution to eq. (30), at $\alpha = 0$, is

$$u_0 = 2\nu_0 \exp\left[i\frac{\mu_0}{\nu_0}z_0 + i\partial_0\right]\operatorname{sech} z_0, \quad (31)$$

Utilizing $\exp i(kx - \omega_0 t)$ and denoting $k = 2\mu_0$, $a_0 = 2\sqrt{2}\nu_0$ we come to the conventional dispersion relation for the S3 soliton (31), $2\omega_0 = k^2 - a_0^2$. The first in α order corrections in variables μ, υ, $\bar{x}$ and ∂ are (see [10])

$$\frac{d\nu}{dt} = \frac{\alpha}{2}\int_{-\infty}^{\infty}\frac{iu_x^*}{\operatorname{ch} z}\exp\left(-i\frac{\mu}{\nu}z + 2it\right)dz \quad (32)$$

$$\frac{d\mu}{dt} = \frac{\alpha}{2}\int_{-\infty}^{\infty}\frac{\operatorname{sh} z}{\operatorname{ch}^2 z}(iu_x^*)\exp\left(-i\frac{\mu}{\nu}z + 2it\right)dz \quad (33)$$

$$\frac{dx}{dt} = \frac{\alpha}{4\nu^2}\int_{-\infty}^{\infty}\frac{z}{\operatorname{ch} z}(iu_x^*)\exp\left(-i\frac{\mu}{\nu}z + 2it\right)dz \quad (34)$$

$$\frac{d\delta}{dt} = \frac{dx}{dt} - 4(\mu^2 - \nu^2) + \frac{\alpha}{2\nu}\int_{-\infty}^{\infty}\left(\operatorname{ch}^{-1} z - \frac{z\operatorname{sh} z}{\operatorname{ch}^2 z}\right) \quad (35)$$
$$\cdot(iu_x^*)\exp\left(-i\frac{\mu}{\nu}z - i\delta + 2it\right)$$

Using relation $\nu = \text{const.}$ one can find

$$\frac{d\mu}{dt} \sim \alpha\int(u_x^{*}2 + u_z^2)\,dz \sim \frac{dP}{dt}$$

The final expression for μ_0, $\bar{x}_0$, δ_0 and ν_0 are

$$\nu = \nu_0 = \text{const.},$$

$$\frac{d\nu}{dt} = -\frac{4}{3}\alpha(\mu^2 + \nu^2)\frac{r}{\operatorname{sh} r}\cos 2(\delta - t), r = \frac{\mu\pi}{\nu},$$

$$\frac{d\delta}{dt} = 4(\mu^2 + \nu^2) + 2\alpha\nu\left[\frac{\mu}{\nu} + \frac{\nu}{3\mu}\left(1 - \left(1 + \frac{\mu^2}{\nu^2}\right)\frac{r}{\operatorname{th} r}\right)\right]$$
$$\times\frac{r}{\operatorname{sh} r}\sin 2(\delta - t)$$

These equations may be solved by an iteration procedure to give in the simple case $\mu_0 < \nu_0$ or ultimately

$$\tilde{\phi} = \exp\left\{-i\left[\left(1 - m\frac{a_0^2}{2}\right)t + \frac{\alpha a_0^2 x}{6}\sin 2t\right]\right\} \quad (36)$$
$$\times\frac{a_0}{\operatorname{ch}\dfrac{a_0}{\sqrt{2}}\left(x + \dfrac{\alpha\cos 2t}{2}\right)}$$

This "solution" satisfies the eq. (33) with accuracy $O(\alpha a_0, a_0^2)$. Equation (32) cannot be satisfied by "solution" (36), even in the leading order in the small parameter αa_0.

The fact that a perturbation in the nonlinear equation can lead to a functional dependence on the coordinate, unlike the non-perturbated one, is quite natural (see, e.g., [11]).

VI. Finally, we describe time-independent soliton-like solutions. Introducing variables $\xi = x - vt$ and $\eta = kx - \omega t$ so as $A(\xi)$ and $\theta(\eta)$ we find that instead of (35) we get

$$-VA_\xi - \alpha A_\xi \sin 2\theta - \alpha k A\theta_\eta \cos 2\theta + \kappa^2 A\theta_{\eta\eta} = 0$$
$$kVA\theta_\eta + A_{\xi\xi} - A + A^3 - Ak^2\theta_\eta^2 + \alpha A_\xi \cos 2\theta = 0$$

If the phase and group velocities coincide $V_{ph} = V_{gr}$ then $\eta = k_\xi$ and the first of eq. (37) may be integrated to give

$$A^2\left(\theta_\xi - \frac{V}{2} - \frac{\alpha}{2}\sin 2\theta\right) = \text{const.} \quad (37)$$

Letting const. $= 0$ by virtue of the soliton boundary condition we have

$$2(V^2 - \alpha^2)^{-1/2}\operatorname{arctg}\frac{V\operatorname{tg}\theta + d}{\sqrt{V^2 - \alpha^2}}, \quad V^2 > \alpha^2$$

$$\xi + C = -V^{-1}\operatorname{tg}\left(\phi - \frac{\pi}{4}\right), \quad V^2 = \alpha^2$$

$$(\alpha^2 - V^2)^{-1/2}\ln\frac{V\operatorname{tg}\phi + \alpha - \sqrt{\alpha^2 - V^2}}{V\operatorname{tg}\phi + \alpha + \sqrt{\alpha^2 - V^2}}, \quad V^2 < \alpha^2$$

The properties of solutions obtained may be exposed on the example of a soliton at rest $V = 0$. In this case the phase,

$$\theta_+ = \pi n + \frac{\pi}{2}$$
$$\theta = \sigma + \theta_0 \equiv \operatorname{arctg} e^{\alpha(x - x_0)} + \theta_\pm \quad (38)$$
$$\theta_- = \pi n, n = 0, \pm 1, \ldots$$

[5] It means that to obtain solution (20) we neglected the terms proportional to $\alpha^2 a_0^2$ and αa_0^3 compared with unity and left the terms $\sim\alpha a_0$ and $\sim\alpha$.

4. PentaMath

PentaMath is a superior program that can substantially contribute to productivity in operations that set a lot of mathematical or statistical work. In user tests, we've proven conclusively that PentaMath outperforms other composition systems by three to one. The page of math shown here took 50 minutes (including four minutes of computer time) to set in its entirety using PentaMath.

PentaMath is simple to use (less employee training time required); it automatically calculates font sizes, placement of copy, rules, radicals, up to the fifth level of superior or inferior, summation, and breaking of equations within text. It draws on 255 displayable characters before getting into the pi mode. And it uses far less terminal screen space, because the command codes are so simple, than do other programs that purport to set math automatically.

While ordinary systems require two to three clean-ups, which tie up the terminal and take a disproportionate amount of operator time, PentaMath *automatically* centers equations within the line measure established for the document. The result: maximum efficiency from minimal effort.

5. Pi Characters

The tedious steps of getting pi characters when you don't have a Penta system, go like this:

a) determine which font the character is on from the font layout chart
b) make sure it is the same type font family
c) determine which shift the pi character is on
d) determine which key the character is accessed by
e) go back to unshift position
f) return to the text font being used.

To accomplish pi characters with a Penta system AutoSort Program, all you key is three characters: semicolon, followed by the easy Penta logic mnemonic for that character. Taking time-on-task as a measure of productivity, Penta's pi character program is clearly the superior one, or ;s1.

Example of AutoSort

Character to Set	*Mnemonic*	*Result*
Small bullet	;sb	•
Large bullet	;lb	●
Ballot box	;bb	☐
Ballot x	;bx	☒
Ballot check	;bc	☑
Number sign	;ns	#
Register mark (sup.)	;rm	®
Commercial A (at)	;ca	@
Minus sign	;ms	−
Times sign	;ts	×
Divided by	;db	÷
British pound (sterling)	;bp	£
Greek cap Sigma	;gS	Σ
Greek l.c. pi	;gp	π
Superior 1	;s1	^{1}
Inferior 9	;i9	$_{9}$

6. Tabular Matter

Keyboarding tables can really slow down an operator, given the amount of mark-up, the proneness to error, the difficulty of correcting, and the laboriousness of counting characters and eyeballing copy measurements that in most systems passes for tabulation.

Penta's tab program gives instant productivity gains — there's less mark-up; keyboarding is done horizontally *or* vertically in columns, which makes the process more closely follow operator logic; there is less chance of error and errors can be more easily rectified because there are fewer codes, and tables are displayed in tabular format on the PentaVue terminal; and the end result is as consistent and logical as Penta programming can make it. Not to mention quick and painless.

FRACTIONAL HORSEPOWER MANUAL STARTERS

WITH MELTING ALLOY TYPE THERMAL OVERLOAD RELAY

Type F fractional horsepower starters provide overload protection as well as manual "on-off" control for small motors in a variety of industrial and commercial installations. Available in one or two pole versions, these devices are suitable for use with ac single phase motors to 1 hp. Two pole starters can also be used with dc motors to 3/4 hp. Typical applications include fans, conveyors, pumps, and small machine tools.

CLASS 2510 2512

- 1 or 2 Pole
- Optional Pilot Light
- 115-230 Volts
- Reliable Overload Construction
- Complete Line — available with toggle or key operator in wide range of enclosures

Type FG-2 Type FO-2

SINGLE-UNIT TYPES

Type of Operator	No. of Poles	Features	General Purpose Enclosure Surface Mounting NEMA Type 1		General Purpose Flush Mounting (Without Pull Box)						Watertight and Dusttight Enclosure NEMA Type 4		Class I Groups B, C & D & Class II Groups E, F & G Enclosure NEMA Types 7 & 9		Open Type		Number of Thermal Units Required *
					Gray Flush Plate		Standard Stainless Steel Flush Plate		Jumbo Stainless Steel Flush Plate								
			Type	* Price	Type	* Price	Type	* Price	Type	* Price	Type	* Price	Type	* Price	Type	* Price	
BASIC STARTER — CLASS 2510																	
Toggle	1	Standard	FG-1	$24	FF-1	$22	FS-1	$24	.....	.....	.....	.....	.....	.....	FO-1	$20	
		With Pilot Light	FG-1P	36	FF-1p	34	FS-1P	36	FSJ-1P	$42	.....	.....	.....	.....	FO-1P	32	1
	2	Standard	FG-2	28	FF-2	26	FS-2	28	.....	.....	.....	.....	.....	.....	FO-2	24	
		With Pilot Light	FG-2P	40	FF-2P	38	FS-2P	40	FSJ-2P	46	.....	.....	.....	.....	FO-2P	36	1
Key	1	Standard	FG-3	32	FF-3	30	FS-3	32	.....	.....	.....	.....	.....	.....	FO-3	28	
		With Pilot Light	FG-3P	44	FF-3P	42	FS-3P	44	FSJ-3	50	.....	.....	.....	.....	FO-3P	40	1
	2	Standard	FG-4	36	FF-4	34	FS-4	36	.....	.....	.....	.....	.....	.....	FO-4	32	
		With Pilot Light	FG-4P	48	FF-4P	46	FS-4P	48	FSJ-4P	54	.....	.....	.....	.....	FP-4P	44	1
STARTER WITH HANDLE GUARD/LOCK-OFF — CLASS 2510																	
Toggle	1	Standard	FG-5	$28	✆		✆	.....	✆	.....	FW-1‡	$ 90	FR-1‡	$ 98	.....	.....	
		With Pilot Light	FG-5P	40	✆		✆	.....	✆	.....	FW-1P‡	122	.....	.....	.....	.....	
		With (2) 3/4" P.T.	.....	.....	.....	.....	.....	.....	.....	.....	FW-1H	98	FR-1H	106	.....	.....	
		With (2) 3/4" P.T. and Pilot Light	.....	.....	.....	.....	.....	.....	.....	.....	FW-1PH	130	.....	.....	.....	.....	1
	2	Standard	FG-6	32	—		—	.....	—	.....	FW-2‡	94	FR-2‡	102	.....	.....	
		With Pilot Light	FG-6P	44	—		—	.....	—	.....	FW-2P‡	126	.....	.....	.....	.....	
		With (2) 3/4" P.T.	.....	.....	.....	.....	.....	.....	.....	.....	FW-2H	102	FR-2H	112	.....	.....	
		With (2) 3/4" P.T. and Pilot Light	.....	.....	.....	.....	.....	.....	.....	.....	FW-2PH	134	.....	.....	.....	.....	1

***Prices do not include thermal units. See ordering information for selection.**
‡Furnished with one 3/4" pipe tap in bottom (reversible for top feed).

FOR ORDERING INFORMATION See Page 176.

DIMENSIONS — Page 178.

✆Order basic starter plus separate handle guard kit.
*To order starter for replacement in Class 2512 device, add suffix letter "T" to type number of toggle operated starter and add **$4.00** to price. (Example: Class 2512 Type FG-22 contains two 2510 FG-2T starters. **$28.00** each).
■Will not fit standard duplex pull box.

7. Command Verification

This is a neat little contributor to productivity. In most automated typesetting systems, a command error either shuts down the system or causes the typesetter to print out garbage. The "remedy" is to take the job off the typesetter, figure out where the mistake is, and fix it; the result is interrupted workflow, and many runs before the first proof-readable copy is generated.

Penta's command verification function finds illegal command-type errors on a single pass, without halting the system. The cursor on the VDT screen clearly points out errors, which can then be corrected without having to pull a job off, or losing any operator productivity.

8. Off-Line Keyboards — and On-Line Keyboards

Keystrokes can be captured by the Penta system using telecommunications technology, floppy disks, or magnetic tape. In systems that use paper tape, work flow is sporadic, constantly being interrupted for the physical movement of work from one station to another. Consequently, nothing happens during those interruptions when operators are waiting for the next thing to happen — with disastrous results in the productivity department.

Even on-line systems, which don't require the physical movement of work, have to command each job individually and separately to proceed to the next function. In other words, work can't be queued. Systems that can queue jobs are frequently incapable of assigning priorities to jobs in the system. Nor can they automatically move from job to job. They need operator intervention in the foreground.

This is where Penta has come up with a real productivity booster called AutoFlow.

With AutoFlow, the Penta system does the work flow and prioritizing (from one to nine can be assigned) in the background mode, a fact which gives the system the clear competitive edge when you consider that the Penta system operator is working *two jobs simultaneously*: one in the foreground, where the operator is getting new work into the system for processing; the other in the background mode, where the AutoFlow feature permits text processing to go on without direct operator intervention.

This operating software for system management eliminates scheduling problems, streamlines the flow of work through the system — and contributes to the productivity of the Penta system as a whole.

9. Search and Replace Program

This complex programming coup allows the system to search for up to 96 strings at a time, replacing them as examined. It is used to find areas in copy where something changes in the overall format or style of the page. An example is searching out spacing in copy that indicates indention for new paragraph. Using a very simple mnemonic, the system automatically finds and changes the format, so that copy flows through with even less operator intervention or interruption.

10. Data Base Program

Exponential productivity gains occur when an already existing data base is processed through the Penta system. To begin with, existing data bases are not re-keyboarded — the system puts in all commands in a fielded magnetic tape. The new formats are easily inserted, and the copy is processed with extreme ease — and major productivity gains.

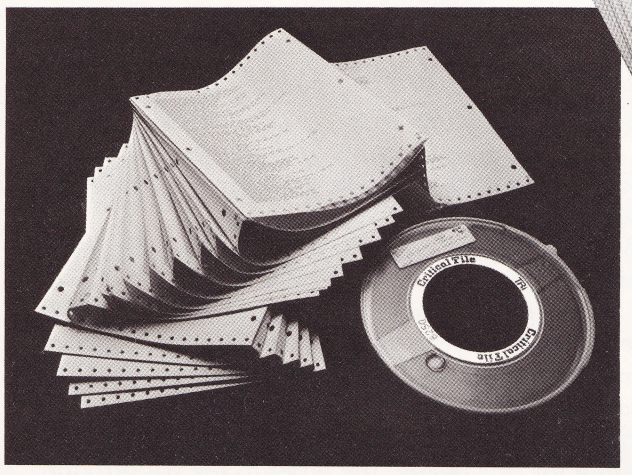

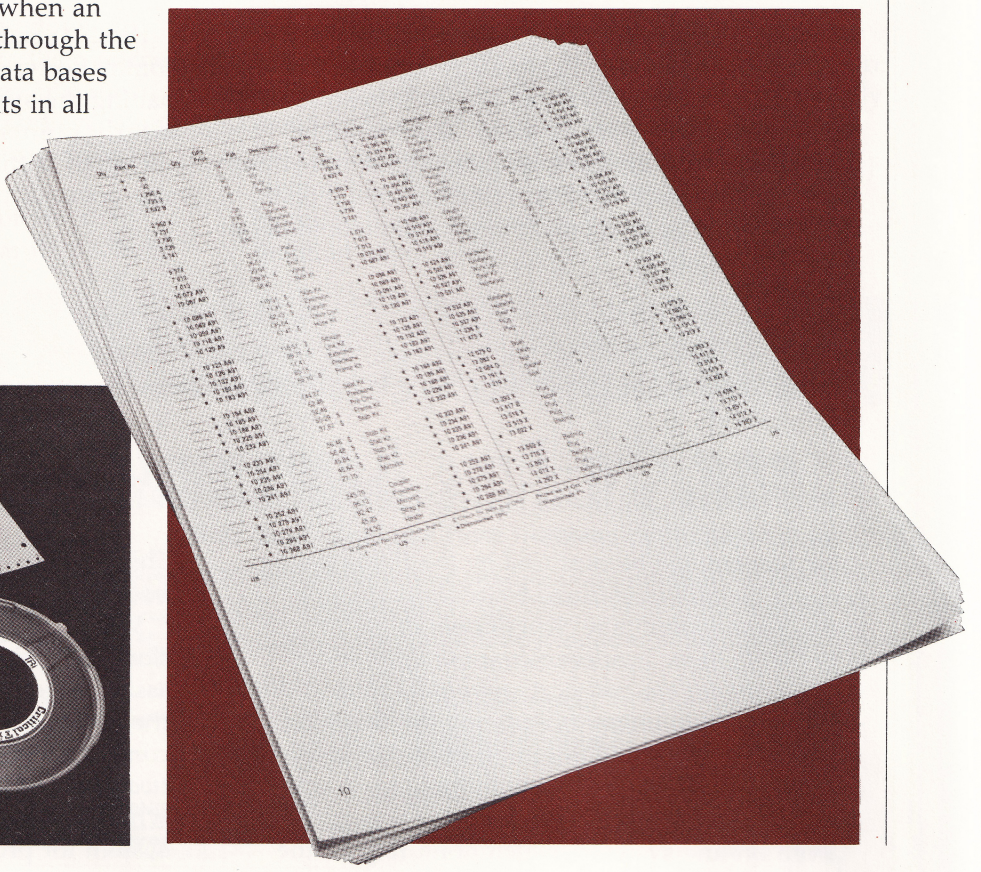

11. Speed

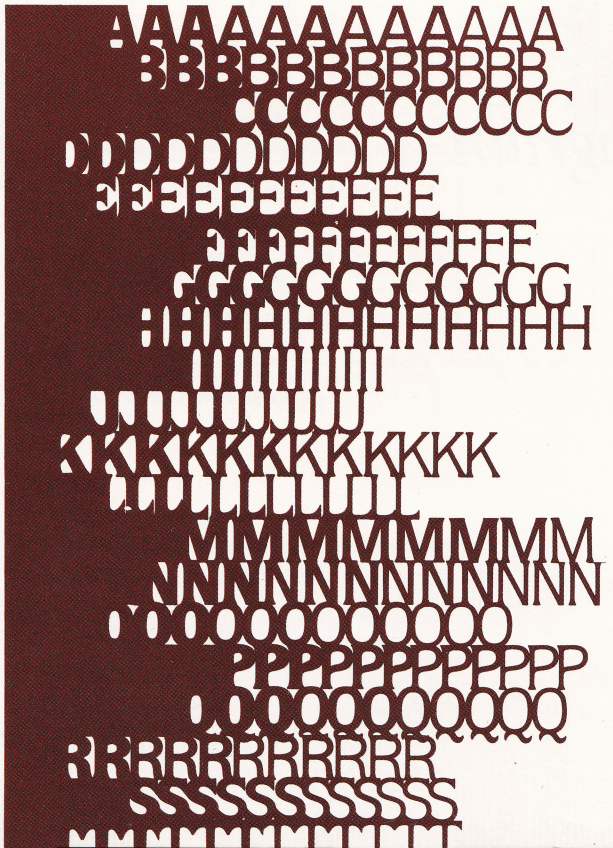

PentaQuick (standard text processing software) coupled with PentaPage gives you the fastest system on the market today — and therefore the most productive. Time tests performed for a major prospect who promptly became a major Penta user (reference on request) proved conclusively that the Penta system is faster than the competition. And more powerful. The tens of thousands of programming and R&D hours we've poured into our systems and software are paying off for over 200 users worldwide. Where productivity is important — and we believe that the company that accomplishes productivity gains will be the company that survives — Penta is there to provide the means.

12. Customer Service

Downtime cripples productivity. All the gains can be wiped out if you don't have access to fast, accurate service. We are dedicated to providing the best customer service in the industry. We consider as essential dimensions of customer service:

- software development
- training of user employees
- software service, at the level the customer requires
- communications.

The extra dimension is the degree to which we care. We want productive users, and we'll go to extraordinary lengths to help your firm get the maximum from your Penta System.

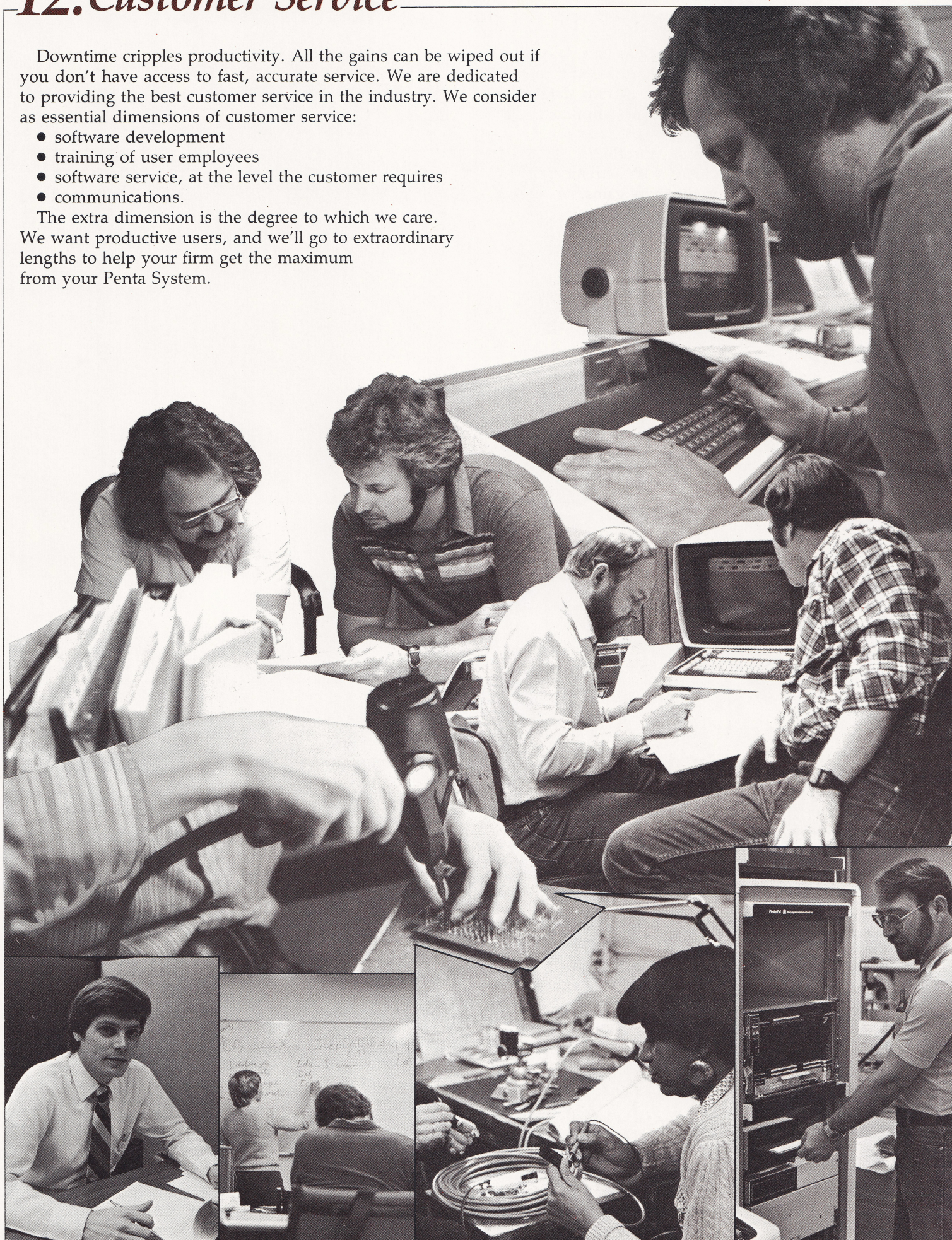

Penta Systems International Inc.

1 EAST CHASE STREET • BALTIMORE, MD 21202 • (301) 244-0050